

Supporting Information for

## **Amorphous Co-doped MoO<sub>x</sub> Nanospheres with Core-Shell Structure Toward Effective Oxygen Evolution Reaction**

Chengying Guo<sup>a</sup>, Xu Sun<sup>a\*</sup>, Xuan Kuang<sup>a</sup>, Lingfeng Gao<sup>a</sup>, Mingzhu Zhao<sup>a</sup>, Liu Qu<sup>a</sup>,

Yong Zhang<sup>a</sup>, Dan Wu<sup>a</sup>, Xiang Ren<sup>a</sup>, Qin Wei<sup>a\*</sup>

a. Key Laboratory of Interfacial Reaction & Sensing Analysis in Universities of Shandong, School of Chemistry and Chemical Engineering, University of Jinan, Jinan 250022, PR China

\*E-mail address: chm\_sunx@ujn.edu.cn; sdjndxwq@163.com

### **Table of contents**

<b>S1. Calculation details.....</b>	<b>2</b>
<b>S2. XRD of CMO and A-MO .....</b>	<b>2</b>
<b>S3. XRD of C-MO .....</b>	<b>3</b>
<b>S4. TEM and SEM images of A-CMO .....</b>	<b>4</b>
<b>S5. EDS spectrum of CMO .....</b>	<b>5</b>
<b>S6. TEM images and catalytic activity characterization of the Co-doped MoO<sub>x</sub> with different reaction time.....</b>	<b>5</b>
<b>S7. Equivalent circuit for modeling the impedance results.....</b>	<b>6</b>
<b>S8. Nyquist plot of various cobalt-doped molybdenum oxides with different Co/Mo ratio.....</b>	<b>6</b>
<b>S9. Cyclic voltammetry curves of C<sub>0.25</sub>MO, C<sub>0.13</sub>MO, CM<sub>0.25</sub>O, CM<sub>0.13</sub>O, A-CMO.....</b>	<b>7</b>
<b>S10. Current density normalized by the C<sub>dl</sub> .....</b>	<b>8</b>
<b>TableS1. Electrocatalytic activity comparison of various molybdenum oxides .....</b>	<b>9</b>
<b>TableS2. Electrochemical analysis based on the current density and the double-layer capacitance .....</b>	<b>9</b>
<b>Reference .....</b>	<b>10</b>

## S1. Calculation details

### Potential vs. RHE calculation:

The measured potentials vs Ag/AgCl were converted to the reversible hydrogen electrode (RHE) according to the following equation:

$$E(\text{RHE}) = E(\text{Ag/AgCl}) + 0.197 + 0.059 \times \text{pH}$$

### Active sites calculation:

Firstly, when measured the polarization curve, record the amount of electricity in the positive and negative directions at a sweep speed of  $5\text{mV s}^{-1}$ . The active sites is calculated by the following formula:

$$\text{active sites (n)} = (Q_+ + Q_-) / (F \times m)$$

m represents the mass loading of electrocatalysts ( $\sim 0.28\text{ mg cm}^{-2}$ ), F is the Faraday constant ( $96487\text{ C mol}^{-1}$ ).

## S2. XRD of CMO and A-MO

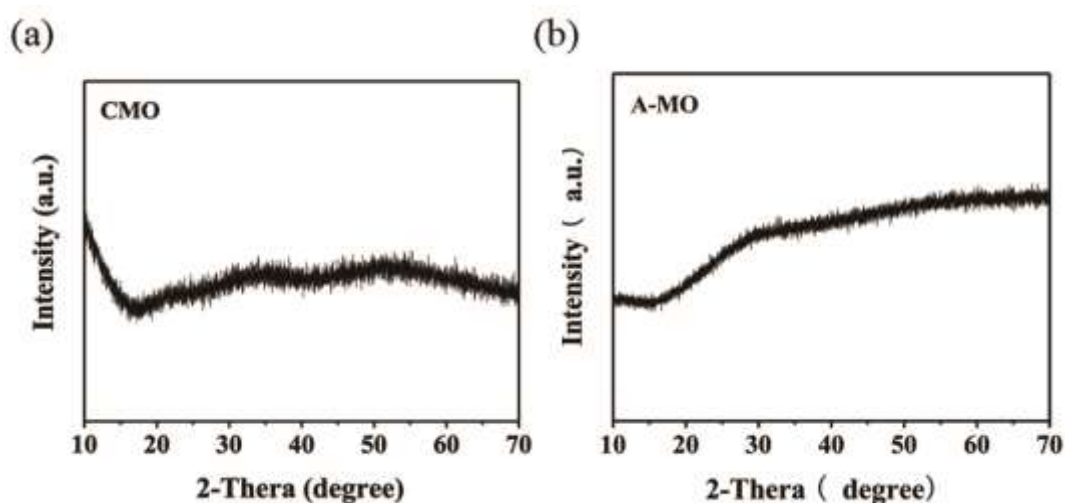


**Figure S1.** XRD patterns of CMO and A-MO. (a) XRD pattern of the as-synthesized CMO. (b) XRD pattern of the as-synthesized A-MO.

### S3. XRD of C-MO

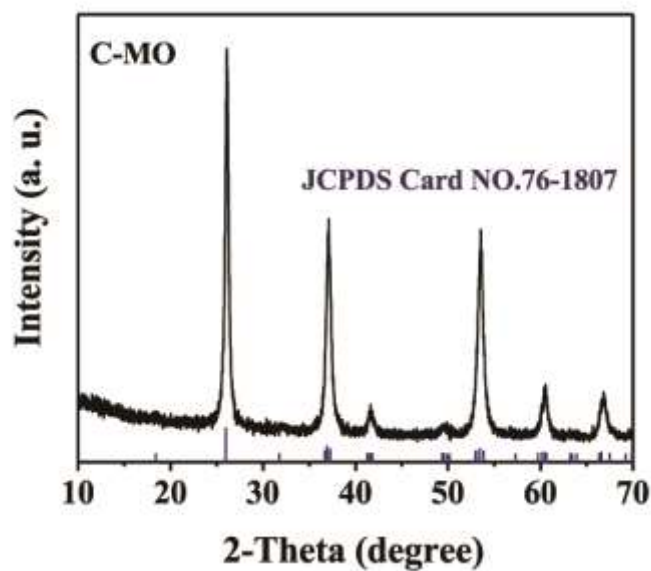


**Figure S2.** XRD pattern of as-synthesized crystalline MoO<sub>2</sub> using the method previously reported.

It can be seen from Figure S2 that all the diffraction peaks of C-MO were in well consistency with MoO<sub>2</sub> (JCPDS Card NO. 76-1807), illustrating the successful fabrication of MoO<sub>2</sub>.

#### S4. TEM and SEM images of A-CMO

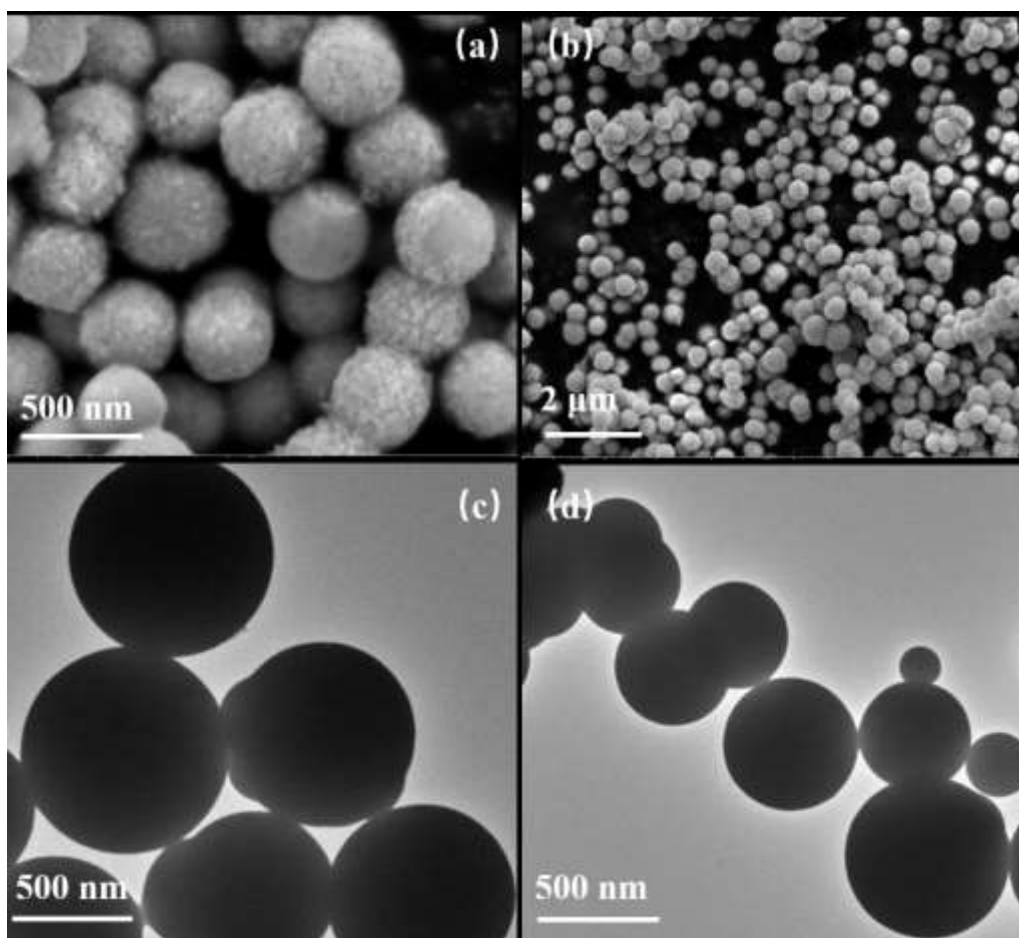


**Figure S3.** (a) and (b) SEM images of the A-CMO. (c) and (d) TEM images of A-CMO.

Figure S3 presented the SEM and TEM images of A-CMO that obtained via the high temperature annealing of CMO in  $N_2$  atmosphere. As can be seen from Figure S3, after annealing treatment, the unique core-shell structure disappeared, with tiny spheres being obtained finally.

## S5. EDS spectrum of CMO

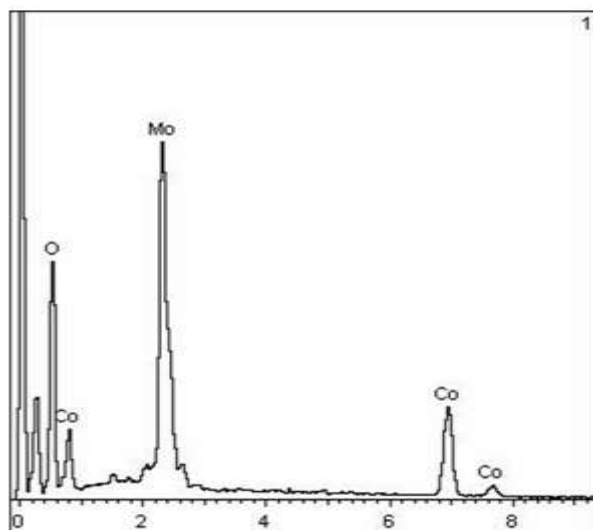


**Figure S4.** EDS spectrum of as synthesized CMO. The successful incorporation of cobalt atoms into the molybdenum oxide was well demonstrated.

## S6. TEM images and catalytic activity characterization of the Co-doped $\text{MoO}_x$ with different reaction time

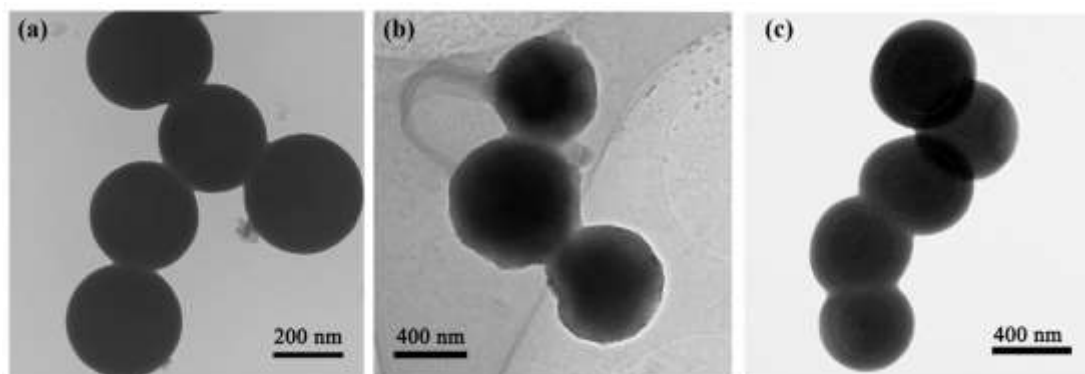


**Figure S5.** Time-dependent experiments of the formation mechanism of the cobalt-doped molybdenum oxides carried out at 180 °C. (a) Solid sphere structures obtained at 1 h. (b) Core-shell structures at 6 h. (c) The obvious core-shell structure of CMO after reacting for 12 h. The formation process is following the well-known Ostwald ripening mechanism.

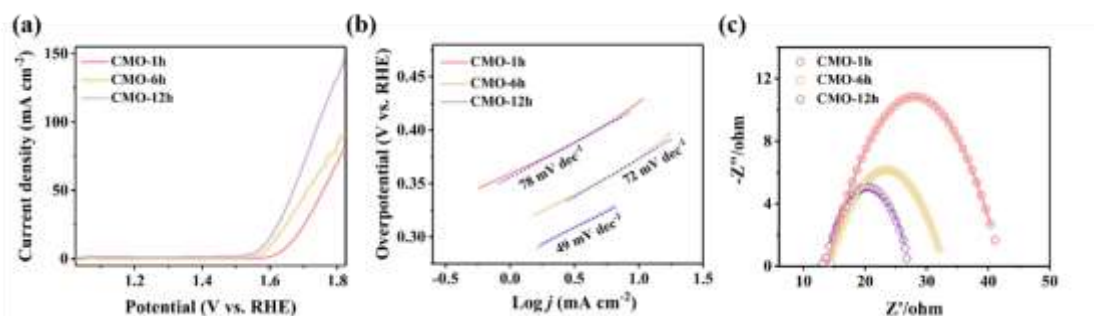


**Figure S6.** Catalytic activity characterization of cobalt-doped molybdenum oxides with different reaction time. (a) Polarization curves of CMO-1h, CMO-6h and CMO-12h. (b) Tafel plots obtained from (a). (c) Nyquist plot of CMO-1h, CMO-6h and CMO-12h. The Co-doped  $\text{MoO}_x$  sample with reaction time of 12h is CMO in manuscripts.

### S7. Equivalent circuit for modeling the impedance results

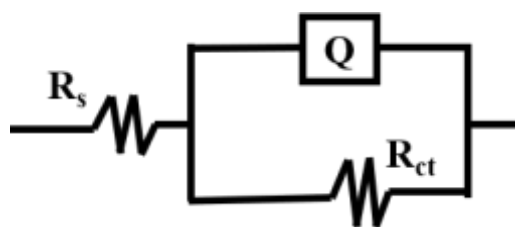


**Figure S7.** Equivalent circuit for modeling the impedance results.

### S8. Nyquist plot of various cobalt-doped molybdenum oxides with different Co/Mo ratio

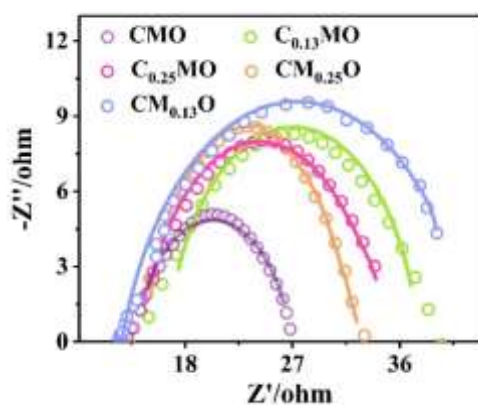


**Figure S8.** Nyquist plot of various cobalt-doped molybdenum oxides with different Co/Mo ratio (CMO,  $\text{C}_{0.13}\text{MO}$ ,  $\text{C}_{0.25}\text{MO}$ ,  $\text{CM}_{0.25}\text{O}$  and  $\text{CM}_{0.13}\text{O}$ ) recorded at a constant potential of 0.65 vs (Ag/AgCl)/V.

**S9. Cyclic voltammetry curves of  $C_{0.25}MO$ ,  $C_{0.13}MO$ ,  $CM_{0.25}O$ ,  $CM_{0.13}O$ , A-CMO**

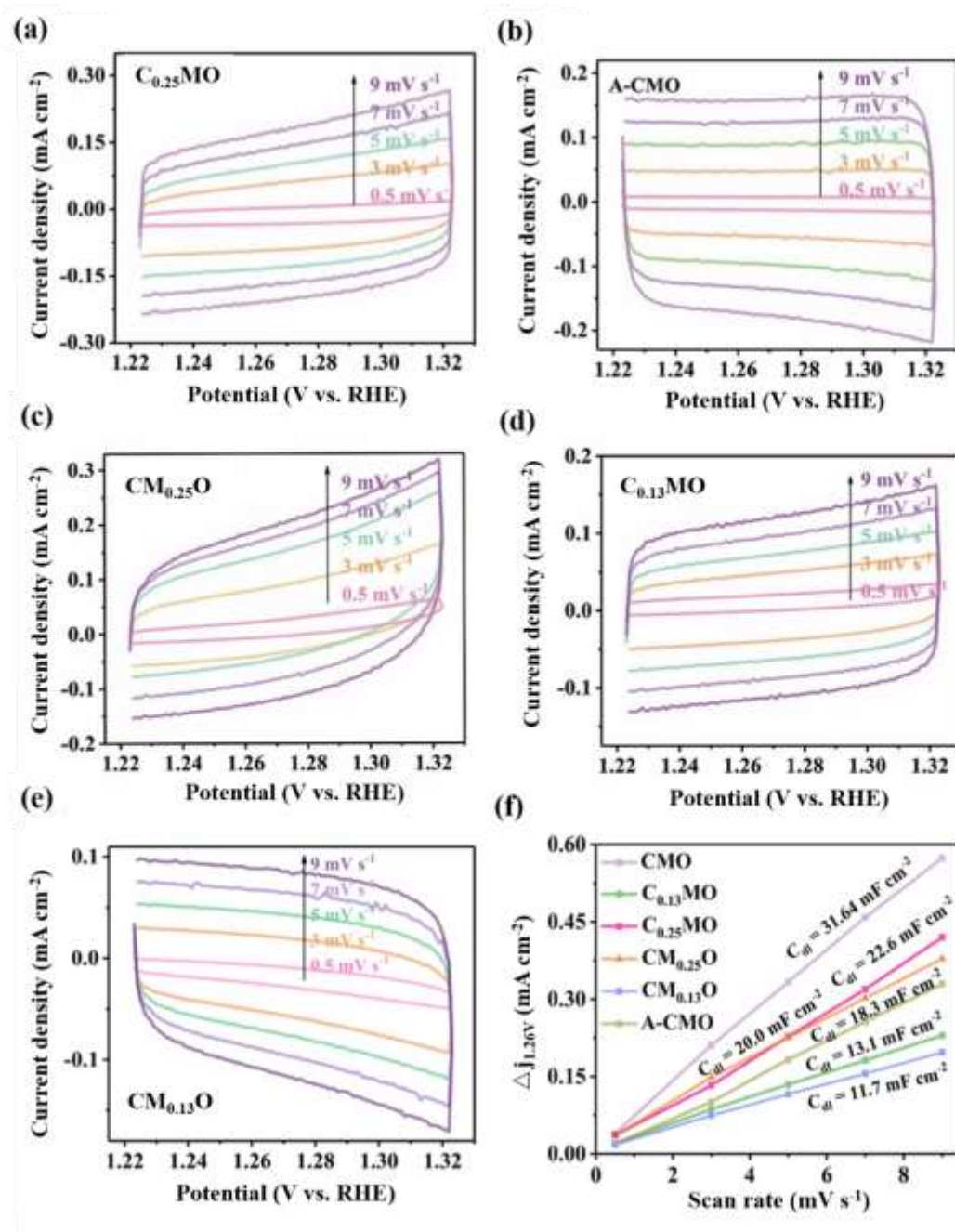


**Figure S9.** Cyclic voltammetry curves of (a)  $C_{0.25}MO$ , (b) A-CMO, (c)  $CM_{0.25}O$ , (d)  $C_{0.13}MO$ , (e)  $CM_{0.13}O$ ; (f) Current density as a function of the scan rate for the different electrodes, from which the  $C_{dl}$  was well calculated.

## S10. Current density normalized by the $C_{dl}$

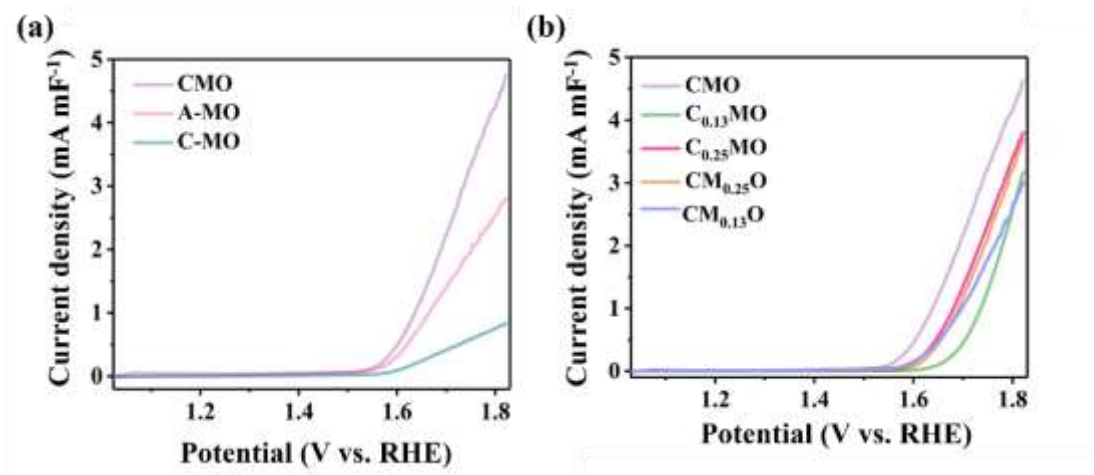


**Figure S10.** Current density normalized by the  $C_{dl}$ . (a) Current density of CMO, A-MO and C-MO normalized by the  $C_{dl}$ . (b) Current density of CMO,  $C_{0.13}MO$ ,  $C_{0.25}MO$ ,  $CM_{0.25}O$  and  $CM_{0.13}O$  normalized by the  $C_{dl}$ .



**TableS1. Electrocatalytic activity comparison of various molybdenum oxides**

	$\eta^a$ / V	$j^b$ / mA cm <sup>-2</sup>	Tafel / mV dec <sup>-1</sup>	$R_{ct}^c$ / $\Omega$	$R_s^d$ / $\Omega$
CMO	0.340	144	49	27	12.57
C-MO	0.567	14	127	335	12.96
A-MO	0.513	22	144	297	13.23
A-CMO	0.382	60	82	125	12.91
C <sub>0.13</sub> MO	0.473	70	74	41	12.83
C <sub>0.25</sub> MO	0.403	99	65	33	12.72
CM <sub>0.25</sub> O	0.415	95	69	37	12.69
CM <sub>0.13</sub> O	0.432	63	106	44	12.89

a: The overpotential value when current density is 10 mA cm<sup>-2</sup>.

b: The current density value when potential is 0.8 V (vs Ag/AgCl).

c: Charge transfer resistance.

d: Series resistor.

**TableS2. Electrochemical analysis based on the current density and the double-layer capacitance**

	$C_{dl}$ / mF cm <sup>-2</sup>	Surface area relative to CMO	<sup>a</sup> Current normalized by $C_{dl}$ / mA mF <sup>-1</sup>	Active sites per surface area relative to CMO	Number of active sites / $\times 10^{-3}$ mol g <sup>-1</sup>
CMO	31.64	1.00	4.64	1.00	6.550
C-MO	1.33	0.04	2.37	0.51	0.194
A-MO	5.13	0.16	2.85	0.61	0.468
A-CMO	18.30	0.58	3.29	0.71	1.077
C <sub>0.13</sub> MO	13.15	0.42	3.63	0.78	2.475
C <sub>0.25</sub> MO	22.61	0.71	3.69	0.80	4.521
CM <sub>0.25</sub> O	20.06	0.63	3.52	0.76	4.478
CM <sub>0.13</sub> O	11.71	0.37	3.18	0.69	3.125

a: Polarization current density normalized by  $C_{dl}$  at 0.8 V (vs Ag/AgCl).

The total relative activity is proportional to the total relative number of active sites, which can be further decoupled as contributions from the relative surface area and the relative density of active sites per surface area<sup>1, 2</sup>:

$$J \propto \text{Surface area} \times \frac{\text{Active sites}}{\text{Surface area}}$$

$$\frac{J}{\text{Surface area}} \propto \frac{\text{Active sites}}{\text{Surface area}}$$

Therefore, the decoupling of the enhanced activity of CMO from contributions due to the surface area versus the density of active sites per surface area would be an efficient way to demonstrate the increment of active sites per surface area.

Via the calculation of CV curves at a region without electrochemical reactions, the  $C_{dl}$  of various molybdenum oxides with or without cobalt doping can be identified. Among all these tested catalysts, the CMO possess a much higher active surface area than the other catalysts, which may arise from the unique core-shell structure and the enhanced conductivity. After normalizing the polarization current density by the  $C_{dl}$ , the influence that the OER activity is enhanced by the enlargement of surface area or conductivity would be excluded, and the activity enhancement can be identified as the result of the high exposure of active sites. As presented in Table S2, after normalizing the current density by the surface area, the number of active sites per surface area of these catalysts determined, among which the CMO shows 2 and 1.6 times increment than that of the C-MO and A-MO, thus directly demonstrating the higher intrinsic OER activity of the nanosheets without concerning the effect of surface area and conductivity.

## Reference

1. J. Kibsgaard, Z. Chen, B. N. Reinecke, T. F. Jaramillo, *Nat. Mater.*, 2012, **11**, 963-969.
2. J. Xie, S. Li, X. Zhang, J. Zhang, R. Wang, H. Zhang, B. Pan and Y. Xie, *Chem. Sci.*, 2014, **5**, 4615-4620.